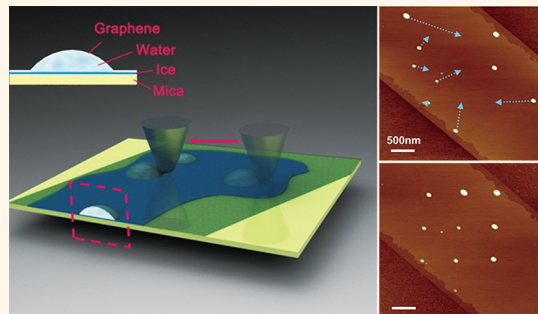


# A Route toward Digital Manipulation of Water Nanodroplets on Surfaces

Meng Cheng,<sup>†,§</sup> Duoming Wang,<sup>†,§</sup> Zhaoru Sun,<sup>†,§</sup> Jing Zhao,<sup>†</sup> Rong Yang,<sup>†</sup> Guole Wang,<sup>†</sup> Wei Yang,<sup>†</sup> Guibai Xie,<sup>†</sup> Jing Zhang,<sup>†</sup> Peng Chen,<sup>†</sup> Congli He,<sup>†</sup> Donghua Liu,<sup>†</sup> Limei Xu,<sup>‡</sup> Dongxia Shi,<sup>†</sup> Enge Wang,<sup>‡</sup> and Guangyu Zhang<sup>†,\*</sup>

<sup>†</sup>Beijing National Laboratory for Condensed Matter Physics and Institute of Physics, Chinese Academy of Sciences, Beijing 100190, China and <sup>‡</sup>International Center of Quantum Materials, School of Physics, Peking University, Beijing 100871, China. <sup>§</sup>M. Cheng, D. Wang, and Z. Sun contributed equally.

**ABSTRACT** Manipulation of an isolated water nanodroplet (WN) on certain surfaces is important to various nanofluidic applications but challenging. Here we present a digital nanofluidic system based on a graphene/water/mica sandwich structure. In this architecture, graphene provides a flexible protection layer to isolate WNs from the outside environment, and a monolayer ice-like layer formed on the mica surface acts as a lubricant layer to allow these trapped WNs to move on it freely. In combination with scanning probe microscope techniques, we are able to move, merge, and separate individual water nanodroplets in a controlled manner. The smallest manipulatable water nanodroplet has a volume down to yoctoliter ( $10^{-24}$  L) scale.



**KEYWORDS:** nanofluidic manipulation · atomic force microscope · graphene cover · ice-like layer · molecular dynamics simulation

Manipulation of water at the nanoscale has recently been of great interest in both theoretical and experimental investigations.<sup>1–6</sup> Much success has been achieved so far through confinement of water in self-assembled nanocontainers,<sup>4,7,8</sup> nanopores, or nanochannels<sup>5,9–12</sup> with a typical volume of an attoliter ( $10^{-18}$  L) or above. In principle, handling individual nanoscale water on certain surfaces, a digital nanofluidic process, could provide more manipulation freedom but face serious difficulties associated with its surface and interface,<sup>4,13</sup> which must be tailored properly. In this study, we show a new route toward manipulation of individual water nanodroplets (WNs) on a mica surface. These WNs are covered by graphene to avoid direct exposure to the environment. Between the WNs and mica surface, there is a lubricant ice-like buffer layer, which allows these WNs to move freely on it under external forces. In combination with scanning probe manipulation techniques, various processes of merging, separating, and patterning of WNs on the mica surface have been achieved under ambient conditions. The volume of the smallest manipulatable WN in our system is around yoctoliter scale,

which is a more than 5 orders of magnitude improvement over the existing micro/nanofluidic manipulation limits.<sup>4–6,11,12</sup>

## RESULTS AND DISCUSSION

Samples were prepared by deposition of mechanically cleaved graphene on muscovite mica in a moist atmosphere, a procedure developed previously for trapping water between a mica surface and graphene.<sup>14,15</sup> Graphite for cleavage is highly oriented pyrolytic graphite (grade ZYA from Materials Quartz, Inc.). Samples were prepared in a glovebox with a relative humidity (RH) of  $\sim 80\%$ , but it was not necessary; lower RH also works well. Figure 1a shows an atomic force microscope (AFM) image of a typical sample with several trapped WNs and an ice-like water layer coexisting around them. The height profiles of a nanodroplet and the ice-like layer along the line-cut indicated by the red and blue lines in Figure 1a are shown below, respectively. We can see that the WN has a spherical-cap shape with a basal diameter ( $D$ ) of  $\sim 330$  nm and net height ( $H$ ) of  $\sim 7.4$  nm, and the 0.4 nm thickness of the ice-like layer is consistent with the monolayer nature of ice.<sup>14,16,17</sup>  $D$  and  $H$  of many WNs covered

\* Address correspondence to gyzhang@aphy.iphy.ac.cn.

Received for review February 13, 2014 and accepted March 19, 2014.

Published online March 19, 2014  
10.1021/nn500873q

© 2014 American Chemical Society

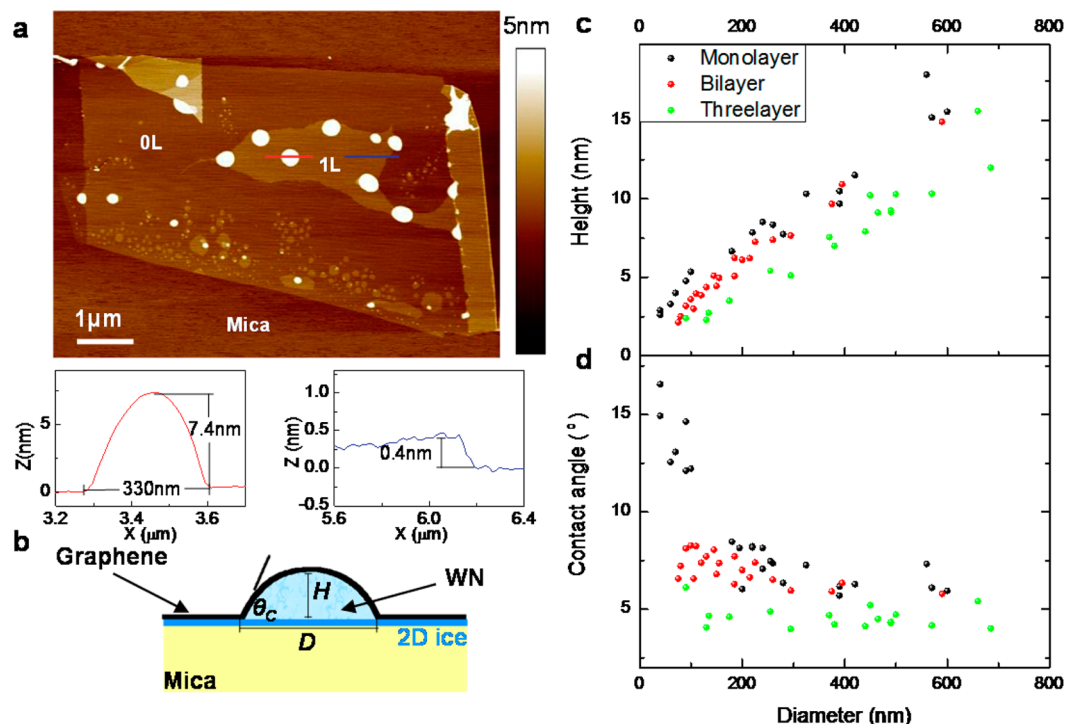


**Figure 1.** Topography of the WNs. (a) AFM image of some WNs trapped between few-layer graphene and mica. The area marked with 0L means graphene contacts with bare mica, and 1L stands for one ice-like layer existing between them. Bottom diagrams give the height profile along the red line and blue line, respectively. (b) Sketch map showing the sandwich structure and the geometry relation of  $H$ ,  $D$ , and  $\theta_c$ . (c)  $D$ – $H$  relationship measured from more than 50 WNs covered by monolayer (black), bilayer (red), and (d) their corresponding contact angles as a function of diameter.

with different layers of graphene were measured and plotted in Figure 1b. For WNs covered by the same layer number of graphene,  $D$ – $H$  shows a linear relationship, while WNs with the same  $D$  have a decreased  $H$  if covered by a thicker graphene layer, which is attributed to the higher in-plane tension of the thicker graphene (Figure 1c). We also calculated the contact angle ( $\theta_c$ ) as a function of  $D$  (Figure 1d; see more discussions in the Supporting Information). We can see that the  $\theta_c$ – $D$  shows an opposite trend as compared with the case for normal micro/macroscale water droplets.<sup>13,18</sup> In our samples, most  $\theta_c$  values were distributed in the range 6–18°, in contrast to ~22.7° for a WN on mica without graphene covering.<sup>19</sup> Note that the  $\theta_c$  of WNs confined between graphene and hydrophobic substrates is 5–12° in previous studies,<sup>18</sup> which is consistent with our results. This similarity indicates that  $\theta_c$  of these trapped WNs should be dominated by the constraint of graphene, rather than the contact line tension.<sup>20</sup> More details on the elastic modulus of the WNs are provided in the Supporting Information (Figures S2, S3).

These WNs along with the surrounding ice-like layer trapped under graphene are very stable; no visible changes were observed during a two-month monitoring period when putting such samples in ambient conditions. In this sandwich structure, the covered graphene, an atomically thin material, is flexible, robust, and hydrophobic, allowing the probing and manipulation of the

underneath WNs directly. Figure 2a illustrates a process of moving the trapped WNs under graphene when we applied a sufficient external force by an AFM tip. Due to this AFM-based manipulation technique (see more details in Methods), we can pattern randomly distributed WNs into regular arrays (Figure 2b,c), merge two or more isolated WNs into a single one (Figure 2d,e), and separate one WN into two or more WNs (Figure 2f). The blue dashed arrows marked in Figure 2b show the routes of the tip during the manipulation process. Throughout the whole process, we had not observed any damage to the graphene, ice-like layer, or mica surface, revealing the robust nature of this structure. It is also worth mentioning that the nanodroplet can follow the designed route well at a tip speed of <100 nm/s, while pulling off of a small WN would occur if the tip speed is >~500 nm/s. Figure 2f shows the isolation of an ultrasmall WN (in the blue dotted circle) from a large one. This separated WN has a  $D$  = ~45 nm and  $H$  = ~1.7 nm, equivalent with a volume of ~1.2 yoctoliter ( $10^{-24}$  L). Such a small amount of volume of liquid cannot be produced or even approached by previous systems in which a typical manipulatable volume is around a femtoliter ( $10^{-18}$  L).<sup>4,21</sup> The isolated WNs in our system could be transported freely to anywhere within a two-dimensional channel enclosed by monolayer ice and graphene, suggesting an advanced nanofluidic process as compared with extensively employed nanofluidic systems based on

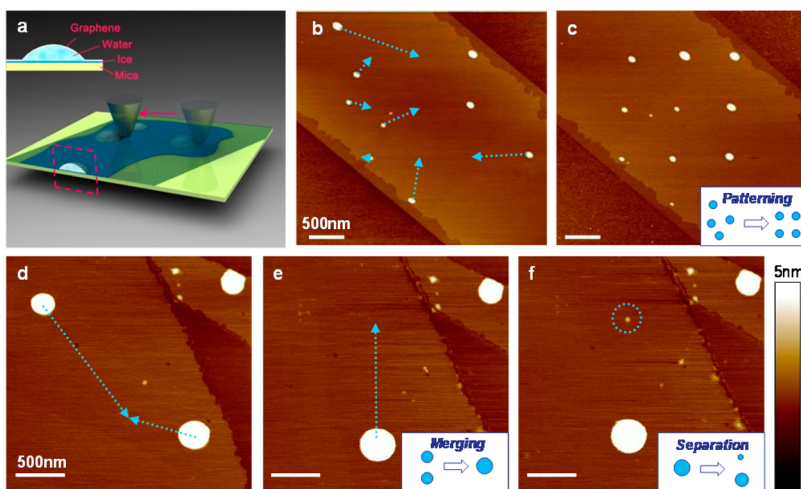


**Figure 2.** Manipulation of WNs. (a) Schematic for the manipulation of a WN by an AFM tip. Inset shows the sandwich structure of graphene/WN/mica. (b and c) With a multistep translation, the disordered nanodroplets are rearranged into an ordered  $3 \times 3$  array. The blue dotted arrow (the same below) represents the path of the tip we preset. (d and e) Two nanodroplets are moved to the same location and merged. (f) An ultrasmall nanodroplet with volume as small as 1.2 yoctoliter is separated from a big one in (e). Inset images of (c), (e), and (f) are the sketches for corresponding processes of the manipulation.

nano pores/nano channels.<sup>5,9–12</sup> This new nanofluidic platform is digital, *i.e.*, dealing with individual WNs.

Control experiments were also carried out to understand the mechanism of the dynamic process of WNs during operation. As shown above, all manipulations for trapped WNs were performed with the ice-like buffer layer around them. In control experiments, we tried to move the WNs without the surrounding ice-like layer (Figure 3a) and found that the WN could not be moved no matter how large the tip indentation force ( $f_{tip}$ ; see more details in Methods) (Figure 3b). Moreover, we also pushed a WN out of an ice-like layer's edge (Figure 3c) and found that the WN would be stuck at the edge (Figure 3d). During the moving of the WNs along a certain trace on the ice-like layer, continuous exfoliation of graphene/ice and intercalation of WNs would occur. These control experiments indicate that the WNs intercalating between graphene and the bare mica surface is not favorable, which is attributed to higher interaction of graphene/mica than that of graphene/ice.

We also performed molecular dynamics (MD) simulations on water confined between mica and graphene to elucidate the mobility of WNs, which was related to the surface and interface in this system. The CLAYFF force field and Lennard-Jones (LJ) potential<sup>22–24</sup> were employed in our simulations (see more details in Methods). With excess water confined between mica and graphene with a separation distance of  $d_0 = 10 \text{ \AA}$ , a dynamically stable WN and a surrounding ice-like layer could be formed (Figure 4a). This ordered monolayer of water molecules has strong binding to the mica surface by forming hydrogen bonds with oxygen atoms on the mica surface. However, this ice-like layer is rough due to the existence of  $\text{K}^+$  ions on the mica surface, making it difficult to form hydrogen bonds with the above WNs (Figure 4a,b). A huge difference was found for the

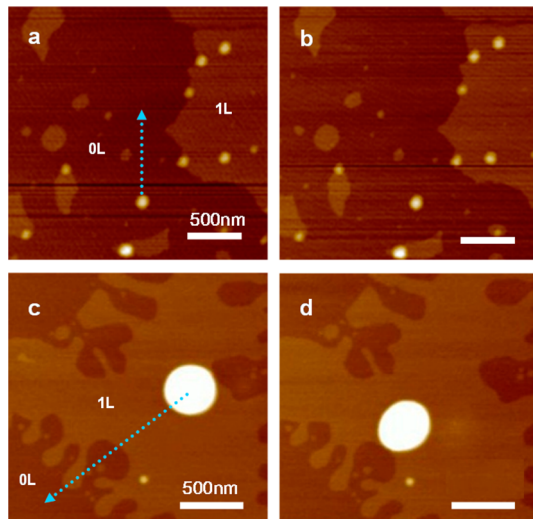


**Figure 3.** Control experiments of WN manipulation. (a) AFM image of the original sample with nanodroplets both on bare mica and the ice-like layer. (b) The nanodroplet on bare mica stays still after being pushed by the AFM tip. (c and d) The nanodroplet on the ice-like layer stops by the edge of the ice-like layer though the tip path extends out of the ice region.

calculated interaction energies between WN/ice ( $\sim 4.26 \text{ kJ/mol}$ ) and mica/ice ( $\sim 34.3 \text{ kJ/mol}$ ). Thus, this ice-like layer acts as a lubricant layer, which allows the WNs to move on it. In addition, the graphene is also hydrophobic and slippery for WNs.<sup>25,26</sup> As a result, both the upper and lower interfaces of the trapped WNs make the nanofluidic process feasible. We further simulated water molecules confined within a mica surface with/without  $\text{K}^+$  ions and a buckled graphene (Figure 4c) and found similar results. As the buckled graphene was moved toward the mica surface, water molecules could move into the bump of graphene, where the separation between mica and graphene was larger.

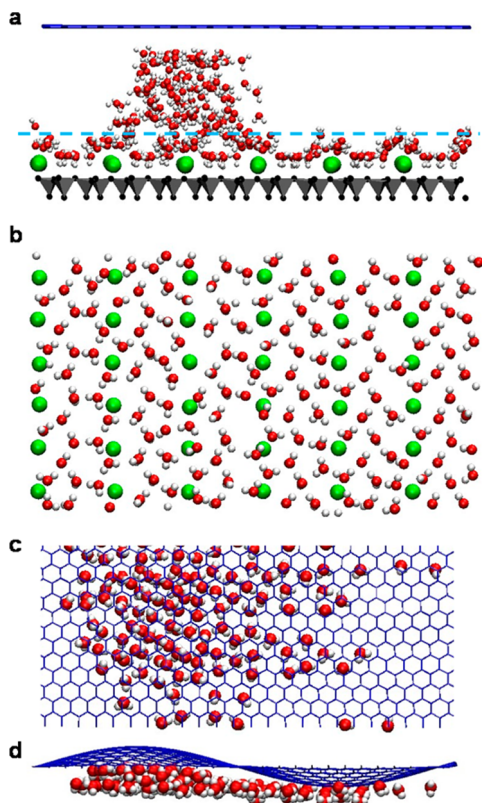


**Figure 4.** Molecular dynamics simulations of water confined between graphene and mica. (a) Side view of water molecules after a 15 ns equilibration run. The temperature is 200 K, corresponding to room temperature (see Supporting Information). The result presents an ice-like layer nearly without free OH bonding. The first tetrahedral structure (Si-Al) of mica is shown in gray triangular polyhedra with black circles representing O atoms, and graphene is shown on the top. The top view of the ice-like layer (under the blue dashed line in a) is shown in (b). (c, d) Top and side view of water molecules confined within mica and buckled graphene after a 10 ns equilibration run; for simplification, mica is not shown. There are more water molecules at the bump of graphene.

In our simulations, the monolayer ice next to mica is very stable (Figure 4). It was noted that stable bilayer and trilayer ice-like structures were reported by previous studies.<sup>14,15,27</sup> Therefore, the stability of the second water layer is possibly related to the local confinement between graphene and mica. In order to confirm this, we carried out contact mode AFM imaging of which the  $f_{tip}$  was large enough to cause significant deformation of the WNs during scanning. In Figure 5, we present a series of images of three WNs with varying  $f_{tip}$  from 20 to 240 nN. Interestingly, a halo of aqueous layer with a thickness of ~0.7 nm (refer to mica) around the droplet appears and grows up gradually with increasing  $f_{tip}$  (Figure 5a–f). Eventually, these nanodroplets vanish at

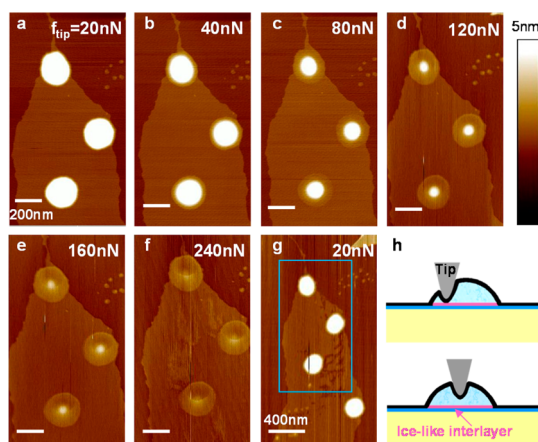


**Figure 5.** AFM images of WNs in contact mode with different tip indentation forces. AFM tip indentation forces during scanning in (a)–(f) are ~20, ~40, ~80, ~120, ~160, and ~240 nN, respectively. (g) Setting the  $f_{tip}$  back to 20 nN and getting a zoom-out image after this series of scanning. (h) Schematic structure of a trapped WN at the moment of contact mode scanning. Different parts of the WN present different deformation degree under a given  $f_{tip}$ . The bottom of this nanodroplet (pink ribbon) is an ice-like layer, also the second ice layer above mica.

$f_{tip} = 240$  nN with only a disk of ice-like bilayer left (Figure 5f). These mirage images can be recovered to normal ones once  $f_{tip}$  is set back to 20 nN (Figure 5g) or below. As AFM is a scanning imaging approach with each pixel representing the local mechanical information, these mirage images reflect a locally stable ice-like bilayer between graphene and mica during the squeezing of WNs by an AFM tip, as illustrated in Figure 5h. Note that the  $f_{tip}$  in the contact mode scanning is much smaller than that for manipulations in tapping mode, causing no WN movement but only deformation.

## CONCLUSION

In conclusion, water nanodroplets trapped between the mica surface and graphene are demonstrated to be a new platform for digital nanofluidics. With the assistance of a graphene protection layer and ice-like lubricant monolayer, these water nanodroplets can be moved, merged, separated, and patterned into regular arrays freely within a two-dimensional channel. The smallest manipulatable WN has volume around 1 yoctoliter. We also employed MD simulations on the structure of this sandwiched platform to understand the interaction at the water/ice interface and the mechanism of manipulation. This new route toward digital manipulation of water nanodroplets on a surface may be applicable in various fields including biology, chemical synthesis, and “lab-on-a-chip” technology.

## METHODS

**Estimation of AFM-Tip Indentation Force ( $f_{tip}$ ).** In contact mode characterization,  $f_{tip}$  could be controlled by adjusting the set

point ( $V_{set}$ ) in the contact mode scanning, which is a voltage signal representing the deflection of the tip.  $V_{preset}$  is the value inputted before tip engaging, which is  $-0.5$  V in our experiment.

The  $f_{\text{tip}}$  can be calculated as  $f_{\text{tip}} = (V_{\text{set}} - V_{\text{preset}})Sk_{\text{tip}}$ , where  $S$  and  $k_{\text{tip}}$  are the sensitivity and spring constant of the tip, respectively. The tip for the experiments presented in Figure 2 is an ESP tip (Bruker Inc. USA) with a spring constant of  $\sim 0.25$  N/m and sensitivity of  $\sim 160$  m/V. As an example, for the picture shown in Figure 3a, the  $V_{\text{set}}$  is 0 V; thus we estimate the  $f_{\text{tip}} = (0 + 0.5 \text{ V}) \times 160 \text{ nm/V} \times 0.25 \text{ N/nm} = 20 \text{ nN}$ . The set points for Figure 2b–f are 0.5, 1.5, 2.5, 3.5, and 5.5 V, respectively.

**AFM-Based Manipulation.** All manipulations were performed by applying the nanolithography function of the Multimode 8 AFM. Tips for tapping mode were used during manipulation, as they are mechanically harsher than other kinds of tips. The script files of Nanoscope software were coded in C++ language. In this script, we could set the parameters such as the depth we pressed the tip into the sample,  $X$ – $Y$  translation distance, and speed of the tip during manipulation. Notice that both the capturing and nanolithography steps were carried out under tapping mode using TESP tips (Bruker Inc. USA). Morphology AFM images were first captured to locate the WN ready for operation. Second the AFM tip was moved to the center of this WN and pushed down a little bit by a few nanometers; then it was moved horizontally along the preset trace. Note that the feedback should be turned off during manipulation.

**MD Simulation.** Water molecules confined between mica and graphene were simulated. The monocrystalline muscovite mica  $\text{KAl}_2(\text{Si}_3\text{Al})\text{O}_{10}(\text{OH})_2$  with a  $6 \times 6$  unit cell in the ( $X$ )–( $Y$ ) dimension and a double aluminosilicate layers in the ( $Z$ )-dimension was used in this study. The supercell of mica is compressed by 6% to match the  $(12 \times 12\sqrt{3})a$  supercell of graphene, where  $a$  is the lattice constant of graphene. The final supercell is  $29.508 \text{ \AA} \times 51.109 \text{ \AA}$  in the  $X$ - and  $Y$ -dimensions, respectively. The  $Z$ -dimension of the supercell is set to  $200 \text{ \AA}$ , to guarantee a separation between graphene and the image of mica of no less than  $150 \text{ \AA}$ . The MD simulations were carried out using the LAMMPS software package<sup>22</sup> with the NVT ensemble. In our MD simulations, we used the CLAYFF force field<sup>23</sup> to characterize the interatomic interactions within mica layers as well as interactions between mica and water. The SPC model<sup>24</sup> was used for water molecules to match the CLAYFF force field. The SHAKE algorithm is applied to keep water molecules rigid. The interaction between water and graphene is described by the 12–6 Lennard-Jones (LJ) potential.<sup>28</sup> The contact angle on graphene is about  $92^\circ$ , which is close to the previous results using first-principle simulations.<sup>29,30</sup> The cutoff distance is  $10 \text{ \AA}$  for LJ potentials and  $9 \text{ \AA}$  for Coulombic potentials, respectively. Since the melting temperature of the SPC water model is  $191 \text{ K}$ ,<sup>31</sup> we simulated water confined within mica and graphene at  $T = 200 \text{ K}$ , which corresponds to room temperature in the real case.

**Conflict of Interest:** The authors declare no competing financial interest.

**Supporting Information Available:** The elastic modulus of the WNs in peak force mode and its dependence on WNs' size; cross section of a water drop in contact mode with different set points. This material is available free of charge via the Internet at <http://pubs.acs.org>.

**Acknowledgment.** This work was supported by the National Basic Research Program of China (973 Program) under Grant Nos. 2013CB934500 and 2012CB921302, the National Science Foundation of China (NSFC) under Grant Nos. 91223204, 61325021, 11204358, and 11174333, and the "100 Talents Project" of Chinese Academy of Sciences (CAS).

## REFERENCES AND NOTES

1. Squires, T. M.; Quake, S. R. Microfluidics: Fluid Physics at the Nanoliter Scale. *Rev. Mod. Phys.* **2005**, *77*, 977–1026.
2. Whitesides, G. M. The Origins and the Future of Microfluidics. *Nature* **2006**, *442*, 368–373.
3. Schoch, R. B.; Han, J. Y.; Renaud, P. Transport Phenomena in Nanofluidics. *Rev. Mod. Phys.* **2008**, *80*, 839–883.
4. Christensen, S. M.; Bolinger, P. Y.; Hatzakis, N. S.; Mortensen, M. W.; Stamou, D. Mixing Subattolitre Volumes in a Quantitative and Highly Parallel Manner with Soft Matter Nanofluidics. *Nat. Nanotechnol.* **2012**, *7*, 51–55.
5. Duan, C. H.; Majumdar, A. Anomalous Ion Transport in 2-nm Hydrophilic Nanochannels. *Nat. Nanotechnol.* **2010**, *5*, 848–852.
6. Napoli, M.; Eijkel, J. C. T.; Pennathur, S. Nanofluidic Technology for Biomolecule Applications: A Critical Review. *Lab Chip* **2010**, *10*, 957–985.
7. Chiu, D. T.; Wilson, C. F.; Rytsen, F.; Stromberg, A.; Farre, C.; Karlsson, A.; Nordholm, S.; Gaggar, A.; Modi, B. P.; Moscho, A.; et al. Chemical Transformations in Individual Ultrasmall Biomimetic Containers. *Science* **1999**, *283*, 1892–1895.
8. Miller, O. J.; Bernath, K.; Agresti, J. J.; Amitai, G.; Kelly, B. T.; Mastrobatista, E.; Taly, V.; Magdassi, S.; Tawfik, D. S.; Griffiths, A. D. Directed Evolution by *in Vitro* Compartmentalization. *Nat. Methods* **2006**, *3*, 561–570.
9. Atencia, J.; Beebe, D. J. Controlled Microfluidic Interfaces. *Nature* **2005**, *437*, 648–655.
10. Huh, D.; Mills, K. L.; Zhu, X. Y.; Burns, M. A.; Thouless, M. D.; Takayama, S. Tuneable Elastomeric Nanochannels for Nanofluidic Manipulation. *Nat. Mater.* **2007**, *6*, 424–428.
11. Kovarik, M. L.; Jacobson, S. C. Attoliter-Scale Dispensing in Nanofluidic Channels. *Anal. Chem.* **2007**, *79*, 1655–1660.
12. Liu, G. L.; Kim, J.; Lu, Y.; Lee, L. P. Optofluidic Control Using Photothermal Nanoparticles. *Nat. Mater.* **2006**, *5*, 27–32.
13. Mendez-Vilas, A.; Jodar-Reyes, A. B.; Gonzalez-Martin, M. L. Ultrasmall Liquid Droplets on Solid Surfaces: Production, Imaging, and Relevance for Current Wetting Research. *Small* **2009**, *5*, 1366–1390.
14. Xu, K.; Cao, P. G.; Heath, J. R. Graphene Visualizes the First Water Adlayers on Mica at Ambient Conditions. *Science* **2010**, *329*, 1188–1191.
15. Cao, P. G.; Xu, K.; Varghese, J. O.; Heath, J. R. Atomic Force Microscopy Characterization of Room-Temperature Adlayers of Small Organic Molecules through Graphene Templating. *J. Am. Chem. Soc.* **2011**, *133*, 2334–2337.
16. Odelius, M.; Bernasconi, M.; Parrinello, M. Two Dimensional Ice Adsorbed on Mica Surface. *Phys. Rev. Lett.* **1997**, *78*, 2855–2858.
17. Teschke, O.; Valente, J. F.; de Souza, E. F. Imaging Two-Dimensional Ice-Like Structures at Room Temperature. *Chem. Phys. Lett.* **2010**, *485*, 133–136.
18. Cao, P. G.; Xu, K.; Varghese, J. O.; Heath, J. R. The Microscopic Structure of Adsorbed Water on Hydrophobic Surfaces under Ambient Conditions. *Nano Lett.* **2011**, *11*, 5581–5586.
19. Spagnoli, C.; Loos, K.; Ulman, A.; Cowman, M. K. Imaging Structured Water and Bound Polysaccharide on Mica Surface at Ambient Temperature. *J. Am. Chem. Soc.* **2003**, *125*, 7124–7128.
20. Degennes, P. G. Wetting - Statics and Dynamics. *Rev. Mod. Phys.* **1985**, *57*, 827–863.
21. Martinez, R. V.; Garcia, R. Nanolithography Based on the Formation and Manipulation of Nanometer-Size Organic Liquid Menisci. *Nano Lett.* **2005**, *5*, 1161–1164.
22. Plimpton, S. Fast Parallel Algorithms for Short-Range Molecular-Dynamics. *J. Comput. Phys.* **1995**, *117*, 1–19.
23. Cygan, R. T.; Liang, J. J.; Kalinichev, A. G. Molecular Models of Hydroxide, Oxyhydroxide, and Clay Phases and the Development of a General Force Field. *J. Phys. Chem. B* **2004**, *108*, 1255–1266.
24. Berendsen, H. J. C.; Postma, J. P. M.; van Gunsteren, W. F.; Hermans, J. Interaction Models for Water in Relation to Protein Hydration. In *Intermolecular Forces*; Pullman, B., Ed.; Reidel Publishing Company: Dordrecht, 1981; pp 331–342.
25. Rafiee, J.; Mi, X.; Gullapalli, H.; Thomas, A. V.; Yavari, F.; Shi, Y. F.; Ajayan, P. M.; Koratkar, N. A. Wetting Transparency of Graphene. *Nat. Mater.* **2012**, *11*, 217–222.
26. Singh, E.; Thomas, A. V.; Mukherjee, R.; Mi, X.; Houshmand, F.; Peles, Y.; Shi, Y. F.; Koratkar, N. Graphene Drape Minimizes the Pinning and Hysteresis of Water Drops on Nanotextured Rough Surfaces. *ACS Nano* **2013**, *7*, 3512–3521.

27. Li, H.; Zeng, X. C. Two Dimensional Epitaxial Water Adlayer on Mica with Graphene Coating: An ab Initio Molecular Dynamics Study. *J. Chem. Theory Comput.* **2012**, *8*, 3034–3043.
28. Hirunsit, P.; Balbuena, P. B. Effects of Confinement on Water Structure and Dynamics: A Molecular Simulation Study. *J. Phys. Chem. C* **2007**, *111*, 1709–1715.
29. Li, H.; Zeng, X. C. Wetting and Interfacial Properties of Water Nanodroplets in Contact with Graphene and Monolayer Boron-Nitride Sheets. *ACS Nano* **2012**, *6*, 2401–2409.
30. Werder, T.; Walther, J. H.; Jaffe, R. L.; Halicioglu, T.; Koumoutsakos, P. On the Water-Carbon Interaction for Use in Molecular Dynamics Simulations of Graphite and Carbon Nanotubes. *J. Phys. Chem. B* **2003**, *107*, 1345–1352.
31. Vega, C.; Abascal, J. L. F. Relation between the Melting Temperature and the Temperature of Maximum Density for the Most Common Models of Water. *J. Chem. Phys.* **2005**, *123*, 144504.